Is Rock-Eval 6 thermal analysis a good indicator of soil organic carbon lability? – A method-comparison study in forest soils

Laure Soucémarianadin, Lauric Cécillon, Claire Chenu, François Baudin, Manuel Nicolas, Cyril Girardin, Pierre Barré

Elsevier Editorial System(tm) for Soil Biology and Biochemistry

Manuscript Draft

Manuscript Number: SBB12198R2

Title: Is Rock-Eval 6 thermal analysis a good indicator of soil organic carbon lability? - A method-comparison study in forest soils

Article Type: Research Paper

Keywords: soil organic carbon kinetic pools; Rock-Eval 6; particulate organic matter; soil basal respiration; deep soil organic carbon; French forest soils

Corresponding Author: Dr. Laure Nalini Soucemarianadin, Ph.D.

Corresponding Author's Institution: Ecole Nationale Supérieure

First Author: Laure Nalini Soucemarianadin, Ph.D.

Order of Authors: Laure Nalini Soucemarianadin, Ph.D.; Lauric Cécillon, PhD; Claire Chenu, PhD; François Baudin, PhD; Manuel Nicolas, PhD; Cyril Girardin, PhD; Pierre Barré, PhD

Manuscript Region of Origin: FRANCE

Is Rock-Eval 6 thermal analysis a good indicator of soil organic carbon lability? – A method-comparison study in forest soils

Laure Soucémarianadin[a,*], Lauric Cécillon[b], Claire Chenu[c], François Baudin[d], Manuel Nicolas[e], Cyril Girardin[c] and Pierre Barré[a]

[a] Laboratoire de Géologie, PSL Research University, CNRS-ENS UMR 8538, Ecole Normale Supérieure, 24 rue Lhomond 75231 Paris CEDEX 5, France

[b] Université Grenoble Alpes, IRSTEA, 2 rue de la Papeterie, 38402 St-Martin-d'Hères, France

[c] AgroParisTech-INRA, UMR ECOSYS, Route de la ferme, 78850 Thiverval-Grignon, France

[d] Sorbonne-Université/UPMC, ISTeP, 4 place Jussieu 75005 Paris, France

[e] Office National des Forêts, R&D, 77300 Fontainebleau, France

* corresponding author: Laure Soucémarianadin, souce@geologie.ens.fr

Abstract

Soil respiration tests and abundance of particulate organic matter (POM) are considered as classical indicators of the labile soil organic carbon (SOC) pool. However, there is still no widely accepted standard method to assess SOC lability and the pertinence of these two time-consuming methods to characterize SOC turnover can be questioned. Alternate ways of determining the labile SOC fraction are thus much needed. Thermal analyses, in particular Rock-Eval 6 (RE6) analysis has shown promising results in the determination of SOC biogeochemical stability.

Using a large set of samples (n = 99) of French forest soils representing contrasted pedoclimatic conditions, including deep samples (up to 0.8 m depth), we compared three different methods used for SOC lability assessment. We explored whether respired-C isolated by a 10-week laboratory soil respiration test, POM-C isolated by a physical SOC fractionation scheme (particle-size > 50 µm and d < 1.6 $g \cdot cm^{-3}$) and several RE6 parameters were comparable and how they correlated.

As expected, respired-C (mg CO_2-$C \cdot g^{-1}$ SOC) and POM-C (% of total SOC) fractions strongly decreased with depth. RE6 parameters showed that SOC from deeper soil layers was also thermally less labile, more oxidized and H-depleted. Indeed, SOC from deeper soil layers had lower proportion of thermally labile SOC, higher $T_{50\_HC\_PYR}$ (temperature at which 50% of the pyrolysable hydrocarbons were effectively pyrolyzed) and $T_{50\_CO2\_OX}$ (temperature at which 50% of the CO_2 gas had evolved during the oxidation phase), larger oxygen index, and smaller hydrogen index. Surprisingly, the two classical indicators of the labile SOC pool (respired-C and POM-C) were only marginally correlated (p = 0.051) and showed layer-specific correlations. Similarly, respired-C was poorly correlated to RE6 parameters. Conversely, the POM-C fraction showed a strong negative correlation with $T_{50\_HC\_PYR}$ (ρ = −0.73) and good correlations with other RE6 parameters.

Our study showed that RE6 parameters were good estimates of the POM-C fraction, which represents a labile SOC pool with a residence time of *ca.* a couple decades that is meaningful regarding SOC stock changes upon modifications in land management. RE6 thermal analysis could therefore be a fast and cost-effective alternative to more time-consuming methods used in SOC pool determination, and may be integrated into soil monitoring networks to provide high-throughput information on SOC dynamics.

Keywords: soil organic carbon kinetic pools; Rock-Eval 6; particulate organic matter; soil basal respiration; deep soil organic carbon; French forest soils;

1. Introduction

Soil organic matter (SOM) degradation has multiple consequences on major soil functions like nutrients cycling, soil emissions of greenhouse gases and affects soil carbon sequestration potential. In particular, the labile part of SOM (turnover < 20 years) is associated with biological (microbial) activity and nutrient cycling (Haynes, 2005) and is very relevant to these issues.

In that context, information on the temporal trajectories of SOC storage at a fine spatial resolution, in the form of detailed mapping of SOC stock evolutions with time for different land management scenarios, are required. SOC dynamics models are the logical candidates to provide such information, but their predictive performance is not yet satisfying, and they would benefit from an improved initialization using fine-scale information on SOC kinetic pools (Luo et al., 2016). Soil monitoring networks have become more prominent in the last twenty years. However, currently they can only provide information relative to the recent temporal (decadal) evolution of total SOC stocks. To use the full potential of these networks and measure the effects of climate and land-use changes on SOC stocks will require indicators of the size of the different SOC pools.

Respiration measurements and particulate organic matter (POM) quantification obtained by various methods of fractionation (particle size only / density only / density + particle-size) (von Lützow et al., 2007) have been used for decades and are now classical estimates of the labile SOC pool.

Laboratory incubations are run under optimum temperature and moisture conditions and use the indigenous microflora. They thus represent a maximum potential rate of C mineralization and an index of C availability in the system, integrating the physical, chemical, and microbiological properties of the soil (Haynes, 2005). Incubations are fairly simple to set-up

but they require space and are time-consuming. Sieving and rewetting also tend to artificially increase the mineralizable pool (Haynes, 1986).

Physical fractionation schemes are easy to implement and do not require expensive equipment although they can become costly when density fractionation is involved. Moreover they are very time-consuming, often requiring multiple and relatively long periods of agitation/settling and drying. The most important limitation is the ability of the fractionation scheme to isolate physical fractions that have homogeneous turnover and thus represent functional non-composite SOC pools (von Lützow et al., 2007).

While respired-C and POM-C fractions both represent a labile SOC pool, the former corresponds to a smaller SOC pool with a shorter mean residence time (usually < 1 year for temperate *in-situ* conditions) (Feng et al., 2016) while the latter corresponds to a larger SOC pool with a longer mean residence time (usually < 20 year for temperate *in-situ* conditions) (*e.g.*, Trumbore et al., 1996; Balesdent, 1996). Because these two methods are both very time-consuming, they cannot address the needs of soil monitoring, *i.e.*, a methodology that is informative, high-yield and relatively cheap to implement, to allow for the analysis of numerous samples.

Among thermal analyses used to characterize SOM, Rock-Eval 6 (RE6) analysis has shown promising results in the determination of SOM biogeochemical stability (*e.g.*, Barré et al., 2016) and thus appears like a good candidate to fill this methodological gap. Originally developed for oil and gas exploration in sedimentary basins, the method was first applied to study soils with hydrocarbons contamination (Lafargue et al., 1998). RE was also shown to provide useful information on SOM originating from soil profiles worldwide (Disnar et al., 2003) and many studies on SOM characterization have been conducted, sometimes using RE analysis in conjunction with other methods like nuclear magnetic resonance (Albrecht et al., 2015), hydrocarbon analysis by gas chromatography (Di-Giovanni et al., 1998), infrared

spectroscopy (Hetényi et al., 2006) or biochemical oxygen demand (Copard et al., 2006) to determine the origin and/or decomposition stage of the organic matter (Hetényi et al., 2005; Sebag et al., 2006).

More recently, RE6 results have been compared with respiration test or SOM fractions at the plot (Gregorich et al., 2015) and the small landscape scale (Saenger et al., 2015) but in both cases the analyses were restricted to superficial soil layers. Gillespie et al. (2014) have also related thermal stability assessed by RE6 to respiration test and X-ray absorption near-edge structure spectroscopy for cryosolic soil profiles (up to 75 cm) in Northern Canada but only in four hummocks. Finally, RE6 thermal analysis has been used to look at SOM dynamics in a sample set with a large soil type variability and some deeper horizons (Sebag et al., 2016), but without comparison to other methodologies.

The objective of this study was to properly "benchmark" RE6 thermal analysis with two classical yet time-consuming methods for labile SOC pool estimation: a soil respiration test isolating a respired-C fraction under controlled laboratory conditions and a physical SOC fractionation scheme isolating a POM-C fraction. We selected soil samples from the French forests monitoring network RENECOFOR at various depths. To our knowledge, this is the first study considering such a large set of samples (covering a wide pedoclimatic variability), including deep soil layers up to 0.8 m. Our sample set thus included soil samples that presumably contained very different proportions of the labile SOC pool. Because the difference in size of the C pool estimated by the respiration test and the POM fractionation (*e.g.*, Haynes, 2005) and the previously observed correlations between stock of labile SOC estimated by RE6 parameters and the POM fraction (Saenger et al., 2015) on one hand and between cumulative C mineralized and a RE6 parameter (Gregorich et al., 2015) on the other hand, we were expecting that: 1/ the results provided by the two classical methods would differ quantitatively while the results from the three methods would be qualitatively

comparable and correlated; 2/ we would be able to derive a significant quantitative relationship between RE6 parameters and the two classical indicators of the labile SOC pool.

2. Material and methods

2.1. Sampling

We considered forest soils samples from 53 permanent forest sites of the French national network for the long term monitoring of forest ecosystems (‘‘RENECOFOR’’), established in 1992 (Ulrich, 1995) by the National Forest Service (ONF; http://www.onf.fr/renecofor) as a part of the European ICP-FORESTS (http://icp-forests.net/) level 2 network (Fig. 1a). They were representative of a good portion the national variability in terms of climate (with MAP and MAT ranging between 703–1894 mm and 4.8–12.3 °C respectively for the 1971–2000 period), soil type (entic Podzol; eutric Cambisol/Calcisol; dystric Cambisol) (IUSS Working Group, 2015) and forest vegetation (coniferous—silver fir; Norway spruce; European larch; Scots pine—and deciduous—beech; oaks *spp*—stands). At each site, samples representing two soil layers were obtained (0–10 cm and 40–80 cm; Fig. 1b). Samples of the top soil layer were composite, at each depth, of 5 × 5 sampling points located over a 5000 m^2 plot, collected between 2007 and 2012 by digging a 50 cm wide soil profile (Ponette et al., 1997; Jonard et al., 2017). Samples of the deeper soil layer were composite from two soil pits located just outside the central plot and collected in 1994–1995 (Brêthes et al., 1997). The surface and deep samples thus originate from two different sampling campaigns. The deep samples were only collected once, during the first campaign, to limit perturbation on the monitoring plots. Basic soil parameters (pH and texture) were determined by Ponette et al. (1997) and are reported as supplementary information (Table SI-A1).

Bulk soils were air-dried and stored in plastic buckets right after sampling. One liter of soil of each layer was retrieved for this study and sieved at 2 mm before analysis.

153

154 2.2. Elemental analysis

155 Bulk < 2 mm-sieved soil samples were ground (< 250 µm; ultra-centrifugal mill ZM 200,
156 Retsch Gmbh) and organic carbon and total nitrogen concentrations were determined by dry
157 combustion with an elemental analyzer (CHN NA 1500, Carlo Elba). Samples with
158 carbonates (total $CaCO_3$ = 3.5–835 $g \cdot kg^{-1}$) were first decarbonated following the same
159 protocol as Harris et al. (2001). Briefly, 30 mg of ground samples were weighed in 5 mm × 9
160 mm silver boats followed by the addition of 50 µL of distilled water. The boats were put in a
161 glass bell jar, next to a beaker containing 100 mL of concentrated HCl (12 $mol \cdot L^{-1}$). The air
162 in the jar was evacuated and samples let to sit in this HCl-saturated atmosphere to allow the
163 acid to dissolve water and hydrolyze the carbonates for 8 h. Then, the decarbonated samples
164 were dried at 60 °C in the silver boats for at least 48 h. Silver boats were further placed in 10
165 mm × 10 mm tin boats and analyzed for C and N.
166 POM fractions (see section 2.4.) were ground with a ball mill (mixer mill MM 200, Retsch
167 Gmbh) or a mortar and pestle when the sample mass was less than 0.05 g. Carbon
168 concentration was determined as for the bulk soil.
169

170 2.3. Respiration test

171 For each sample, 20 g of 2 mm-sieved soil were transferred in a 120 mL glass-flask and re-
172 wetted at pF 2.5 (−0.033 MPa), which had been previously determined using a 5 Bar pressure
173 plate extractor (#1600, Soilmoisture Equipment Corp.). The flasks were fitted with aluminum
174 seals with PTFE-faced silicone septa to allow for headspace gas sampling and placed inside
175 an incubator (AE240 BIO EXPERT, Froilabo SAS) kept at 20 °C for 10 weeks following a
176 two-week period pre-incubation to allow the samples microbial activity to stabilize (data not
177 included).

178 Headspace gases were sampled at 1 to 2-week intervals during the 10-week incubation period
179 and CO_2 concentrations were determined using an Agilent 490 micro-gas chromatograph
180 equipped with the OpenLAB Chromatography Data System EZChrom software.
181 When CO_2 concentrations had reached 2.5–3% or was expecting to do so before the next
182 measurement, and/or when the cap had been pierced with the needle four times, flasks were
183 opened and flushed with fresh and moist air to return CO_2 concentrations to ambient levels to
184 avoid anoxia (while maintaining the moisture content), before returning them to the incubator.
185 The CO_2 concentrations measured by the GC were converted in µ CO_2-C·using equation 1:
186 µg C-CO_2 = mmol air × ppm CO_2 (µmol C/ mol air) × 10^{-3} (mol/mmol) × 12 (µg C / µmol C)
187 (equation 1)
188 where "mmol air" corresponds to the millimoles of air present in the flask and was calculated
189 with the ideal gas law (equation 2):
190 n = PV / RT = (1 × 100) / (82.05 × 293) (equation 2)
191 As a result, we multiplied our concentrations of CO_2 expressed in percent by 499.16 to
192 convert them in µg C-CO_2.
193 Finally, the 10-week mineralizable SOC (respired-C) was expressed in mg CO_2-C·g^{-1} SOC to
194 account for differences in the C content of the various layers and sites.
195

196 2.4. Particle size and density SOC fractionation

197 To isolate the particulate organic matter (POM) fraction, samples were first dried at 50 °C for
198 24 h before weighing 25 g and transferred them in polyethylene (PE) 250 mL flasks. We then
199 added 180 mL of 0.5% sodium hexametaphosphate solution and ten 5 mm-diameter glass
200 beads before shaking the samples overnight (50 rpm; 16 h) on an overhead shaker (Reax 2,
201 Heidolph), in order to breakdown soil aggregates. Samples were thoroughly rinsed over a 50-
202 µm mesh with deionized water. The > 50 µm fraction was then transferred back to a dry PE

flask with a sodium polytungstate (SPT) solution of density = 1.6 ± 0.03 $g \cdot cm^{-3}$ (Golchin et al., 1994; Crow et al., 2007) and the solution was added up to *circa* 180 mL. The flasks were shaken overhead by hand 10 times and samples were left overnight to settle down after the cap of the flask was rinsed with the SPT solution. The floating material was collected with a spatula and placed over a 50-µm mesh sieve. If necessary some SPT solution was added back to the flask and the previous step was repeated. This time, samples were placed in a centrifuge for 30 minutes to accelerate the separation (2750 rpm or 1250 g, Six et al., 1998). The floating material was again collected with the spatula or pipetted depending on the amount left. This step was repeated if the light fraction was abundant. If not, samples were left to settle down overnight before one last collection. The POM fraction on the sieve was thoroughly rinsed with deionized water throughout the whole process. The sieves and fractions were then placed in the oven at 50 °C for 24 h before being weighed. To account for differences in the C content of the different samples, we calculated the proportion of OC in the POM fraction (POM-C), expressed in g POM-C·g^{-1} total SOC.

2.5. Thermal analysis: Rock-Eval 6

The thermal analysis of the samples was performed with a Rock-Eval 6 turbo device (Vinci Technologies, France). Details about the equipment have been previously published (Behar et al., 2001). We adapted the procedure developed for the analysis of soil organic matter by Disnar et al. (2003). Briefly, about 60 (20.7–62.1 depending on the sample's C content) mg of ground sample were exposed to two consecutive thermal treatments, first in a pyrolysis oven (200–650 °C; thermal ramping rate of 30 °C·min^{-1}; under N_2 atmosphere) then in a combustion oven (300–850 °C; thermal ramping rate of 20 °C·min^{-1}; under laboratory air atmosphere). At the beginning of the pyrolysis, there was an isothermal step (at 200 °C) during 180 seconds during which the free hydrocarbons (HC) were thermovaporized (S1

peak). The pyrolysis effluents (mostly HC) were detected and quantified with flame ionization detection, while CO and CO_2 were quantified by infrared detection during both the pyrolysis and oxidation stages (Fig. SI-A1).

Two standard RE6 parameters describing SOC bulk chemistry were determined: the hydrogen and oxygen index values (HI and OI_{RE6}). The HI index corresponds to the amount of hydrocarbons formed during thermal pyrolysis of the sample (HC evolved between 200 and 650 °C minus the S1 peak) divided by the total SOC content of the sample and is expressed in mg $HC \cdot g^{-1}$ SOC. It describes the relative enrichment/depletion of SOC in hydrogen-rich moieties. The OI_{RE6} index describes the relative oxidation status of SOC. It was calculated using the equation proposed by Lafargue et al. (1998):

$$OI_{RE6} = 16 / 28 \times OI_{CO} + 32 / 44 \times OI_{CO2} \quad \text{(equation 3)}$$

Where OI_{CO2} corresponds to the CO_2 yielded during thermal pyrolysis of the sample between 200 and 400°C divided by the total SOC of the sample and OI_{CO} corresponds to the CO yielded during thermal pyrolysis between 200 and 400–650°C (wherever a minimum of CO production is observed; in the absence of a minimum, the default upper-limit temperature is set at 550 °C) divided by the total SOC of the sample. Thus OI_{RE6} is expressed in mg $O_2 \cdot g^{-1}$ SOC.

We derived four additional RE6 parameters describing the thermal stability of SOC: (i) $T_{50\_HC\_PYR}$, the temperature at which 50% of the HC resulting from the SOM pyrolysis had evolved (ii) the $T_{50\_CO2\_OX}$, the temperature at which 50% of the residual SOM was oxidized to CO_2 during the oxidation phase. Because the signal was noisy at the beginning of the pyrolysis, we started the integration for $T_{50\_HC\_PYR}$ right after the S1 peak. For $T_{50\_CO2\_OX}$, the upper limit temperature for signal integration was set at 611 °C to obtain a total CO_2 signal evolved from pure OM without interference of carbonates. Both these T_{50} temperature parameters and the HI index have been previously shown as good thermal indicators of SOM

253 biogeochemical stability (Gregorich et al., 2015; Barré et al., 2016). We also included two
254 thermal indices previously used in the literature: the (iii) R-index or (1 − R400), which
255 correspond to the integrated area of the HC thermogram above 400 °C over the total area of
256 the HC signal (Disnar et al., 2003; Sebag et al., 2016). The R-index estimates the proportion
257 of thermally stable SOC pool and varies between 0 and 1. We hypothesized that the
258 proportion (1 – R-index) would approximate a thermally labile/intermediate (turnover < 20
259 years) SOC pool. Finally, using equation 4, we calculated the (iv) I-index, which is an
260 indicator of the preservation of thermally labile immature SOM (Sebag et al., 2016):
261 $\log_{10}((A1 + A2) / A3)$ (equation 4)
262 where A1 + A2 corresponds to the integrated area of the HC thermogram below 400 °C and
263 A3 the integrated area of the HC thermogram between 400 °C and 460 °C.
264 Signal processing of the RE6 thermograms (signal integration and calculation of the
265 $T_{50\_HC\_PYR}$, $T_{50\_CO2\_OX}$, R and I indices) was performed with the R environment software v.3.3
266 (R Core Team, 2016) using the hyperSpec (Beleites and Sergo, 2015) and pracma (Borchers,
267 2015) R packages.
268

269 2.6. Calculations and statistical analyses

270 For RE6 analysis and the respiration test, samples with very low C content (< 0.2%) were not
271 considered as the carbon flux they produced during the incubation or the thermal analysis was
272 too low/too close to the limit of detection for reliable determination. This resulted in the
273 selection of n = 46 for the soil layer 40–80 cm (total n = 99).
274 The mean values of the variables derived from the SOC respiration test, fractionation and RE6
275 analysis for all layer depths were compared using standard non-parametric statistical methods
276 such as Kruskal Wallis test one-way ANOVA by ranks and Wilcoxon signed-rank test.
277 Relationships between the variables derived from the three methods were estimated using

Spearman rank correlation as the data did not meet the assumption of normality. Correlation tests were first performed on the whole dataset (n = 99) then within the 0–10 cm and the 40–80 cm layers, the three soil types and the two vegetation types individually. All comparisons were considered significant at an alpha value (α) of 0.05. A principal component of analysis (PCA) was performed to detect linear relations between parameters derived from the 3 methods. For that purpose, data were log-transformed, centered and scaled. Because the I-index was negative in some instances, we added the equivalent of the smallest I-index value + 0.2 to all the I-index values to run the PCA. To determine the number of principal components to select, we looked at the percentage of the total variance explained and used a scree plot and Kaiser's criterion. To analyze the relationship between RE-based and the two classical indicators of the labile SOC pool, we used a simple linear regression model and relied on the Cook's distance to identify potential outliers. All statistical analyses were performed using R 3.3 (R Core Team, 2016) using the factoextra (Kassambara and Mundt, 2016) and Hmisc (Harrell et al., 2016) packages.

3. Results

3.1. Respiration test

The 10-week mineralizable SOC (respired-C) was expressed in mg CO_2-C·g^{-1} SOC to account for differences in the C content of the various layers and sites. Over the course of the 10-week incubation, the surface layer (0–10 cm) samples cumulatively respired on average 17 ± 7.2 mg CO_2-C·g^{-1} SOC, while the deeper layer (40–80 cm) samples respired 13.4 ± 6.9 mg CO_2-C·g^{-1} SOC (Table 1). There was a significant decrease in respired-C with depth (p = 0.003), indicating a smaller size of the labile C pool in the deeper layers of our forest soils. Within each soil layer, the large standard deviation (around 7.0 mg CO_2-C·g^{-1} SOC) illustrates an important inter-site variability.

303

304 3.2. POM fractionation

305 The POM-C fraction (% of total C) decreased by half between layers 0–10 cm and 40–80 cm
306 with 22.6 ± 7.3% and 11.0 ± 6.1% respectively. This indicates a significantly ($p < 0.001$)
307 smaller labile C pool in the deeper (40–80 cm) soil layer. POM-C ranged between 12.1–
308 43.0% and 2.5–33.6% in the 0–10 cm and 40–80 cm layers, respectively, illustrating again an
309 important inter-site variability.

310

311 3.3. RE6 thermal analysis

312 There was a significant effect of depth on all RE6 parameters. Particularly, the two T_{50}
313 parameters increased significantly ($p < 0.001$) with depth: 421 ± 9 °C to 448 ± 10 °C and 399
314 ± 9 °C to 431 ± 18 °C (Table 1), for $T_{50\_HC\_PYR}$ and $T_{50\_CO2\_OX}$ respectively, corresponding to
315 an increase in the thermal stability of total SOC (*i.e.* a relative decrease in the labile C pool
316 and increase of the stable C pool). OI_{RE6} showed a similar increasing trend ($p < 0.001$) with
317 depth (225 ± 37–439 ± 138 mg $O_2 \cdot g^{-1}$ total SOC; Table 1), reflecting a more oxidized SOC in
318 the deeper layers. Conversely, HI decreased significantly ($p < 0.001$) with depth (276 ± 77–
319 133 ± 34 mg $HC \cdot g^{-1}$ total SOC; Table 1), suggesting a relative depletion of total SOC in H-
320 rich moieties with increased soil depth. The proportion of thermally stable SOC R-index, also
321 experienced a significant increase ($p < 0.001$) with depth (59–69%; Table 1), while the I-
322 index decreased slightly (0.17–0.11; Table 1).

323

324 3.4. Correlations between methods

325 3.4.1. For all samples

326 There were mainly significant and strong correlations between POM-C and the RE6
327 parameters (Table 2). Notably $T_{50\_HC\_PYR}$, OI_{RE6} and R-index all had a strong negative

correlation with POM-C (Spearman ρ = −0.73, −0.76 and −0.69 respectively; Table 2; Fig. 3). $T_{50\_CO2\_OX}$ and HI moderately correlated with POM-C (ρ = −0.56 and 0.67) and the I-index had a weak positive relationship with POM-C (ρ = 0.35). I-index, $T_{50\_HC\_PYR}$ and R-index were the only parameters that were significantly related to respired-C, with a weak correlation (ρ = 0.32, ρ = −0.26 and −0.31 respectively; Table 2). The two classical methods of estimation of labile SOC (respired-C and POM-C) were weakly positively (ρ = 0.20; Table 2; Fig. SI-B1 a) and indeed only marginally (p = 0.051) related.

To describe the similarity or dissimilarity in the different indicators of SOC lability, we conducted a principal components analysis (PCA). As shown by the correlation test, $T_{50\_HC\_PYR}$ and R-index on the one hand and OI_{RE6} and HI on the other hand were highly correlated (ρ = 0.93 and −0.92 respectively; Table 2). We thus decided to conduct the PCA using only the 6 following explanatory variables = respired-C; POM-C; HI; $T_{50\_CO2\_OX}$; $T_{50\_HC\_PYR}$; I-index). The first two principal components (PC) explained approximately 73% of the total variance, with 53% explained by the first and 20% explained by the second PC, respectively (Fig. 2). PC1 clearly separated surface (0–10 cm) from deeper (40–80 cm) soil samples. Along PC1, POM-C and HI showed moderate negative loadings (−0.47 and −0.46 respectively; Table SI-B1) while $T_{50\_HC\_PYR}$ and $T_{50\_CO2\_OX}$ had moderate positive loadings (0.53 and 0.45; Table SI-B1). Respired-C and the I-index showed strong positive loadings along PC2 (0.55 and 0.69; Table SI-B1), while they showed very weak negative loadings along PC1. Samples from layers 0−10 and 40−80 cm did not significantly differ along the second PC.

3.4.2. For the 0–10 cm and 40–80 cm layer separately

These global correlations prompted us into looking at the influence of soil depth on the different parameters. The paired correlations between the 8 parameters differed in surface (0–

353 10 cm) and deep (40–80 cm) layers (Table 2). Specifically, the respired-C in the surface
354 layers was weakly and negatively related to POM-C ($\rho = -0.29$; Table 2). Conversely in the
355 deep layers, respired-C and POM-C were moderately and positively correlated, as it would be
356 expected ($\rho = 0.47$; Table 2; Fig. SI-B1 a). In the surface layers, HI and OI_{RE6} were also
357 moderately (negatively and positively, respectively; Table 2) correlated to respired-C, while
358 in the deep layers we observed again this negative and moderate correlation between
359 $T_{50\_HC\_PYR}$ and respired-C. For POM-C, we found the same negative correlations with
360 $T_{50\_HC\_PYR}$ and OI_{RE6} as in the "all samples" comparison but they were less strong ($\rho = -0.35$
361 to −0.42; Table 2). In the surface layer, the C/N ratio, pH and clay content had all moderate
362 and significant correlations with respired-C and $T_{50\_HC\_PYR}$ (Table 2). These correlations were
363 absent in the 40–80 cm layer.
364 We also looked at the evolutions of the correlations as a function of vegetation and soil types,
365 but there were no change as drastic as the ones we observed with depth (Table SI-C1). In both
366 cases the changes affected only the correlations between respired-C and the other parameters.
367 For instance, in coniferous plots, respired-C was weakly to moderately positively correlated to
368 clay content ($\rho = 0.27$) and pH (0.37) while those correlations were absent in deciduous plots
369 (Table SI-C1). For the soil types, POM-C and respired-C were moderately and positively
370 correlated in Podzols (0.42) and eutric Cambisols (0.46) but not in dystric Cambisols.
371 Furthermore, in eutric Cambisols, respired-C was moderately and negatively correlated with
372 $T_{50\_CO2\_OX}$ (−0.54), R-index (−0.50) and pH (−0.57; Table SI-C1).
373

374 # 4. Discussion

375 ## 4.1. Relationships between respiration test and POM fractionation

376 Unexpectedly the two classical indicators of the labile SOC fraction correlated only weakly
377 and marginally when considering all our samples.

POM-C is considered as a labile SOC fraction (Wander, 2004; Haynes, 2005; von Lützow et al., 2007), and we thus expected it would correlate significantly and strongly with the respired-C fraction isolated by the 10-week laboratory respiration test. Indeed, in his review, Haynes (2005) mentioned several studies reporting a positive and usually strong correlation between the respired-C and the POM-C fractions, appearing to support that hypothesis. However when carefully considering these papers (Janzen et al., 1992; Hassink, 1995; Campbell et al., 1999a; Campbell et al., 1999b; Wander and Bidart, 2000) and others (Liang et al., 2003; Hassan et al., 2016; Li et al., 2016), it emerged that the presented data were not normalized by the total SOC concentration of the samples. Without normalization it could be argued that the positive correlation between the POM-C and the respired-C fractions was in fact driven by variations in total SOC concentration and not SOC biogeochemical stability. It also prevented comparisons among studies, given the important difference in SOC concentration.

The hypothesis of a positive correlation between the sizes of the labile SOC pool estimated by respiration test and POM fractionation schemes has actually not been properly tested on multiple sites, using SOC normalized data as it has been done in the present study. Indeed, the few studies that have reported moderate to strong positive correlations between the sizes of the labile SOC pool estimated by respiration test and POM fractionation were conducted on similar soils under different management (*e.g.*, Alvarez and Alvarez, 2000) or correlations were made within sites (*e.g.*, Janzen et al., 1992). When combining results from all sites, the correlation appeared to be weaker and it can therefore be hypothesized that in our study the weak and marginally significant correlation between POM-C and respired-C was partially due to the large inter-sites variability of soil properties for our sample set (Table SI-A.1).

Finally, the labile SOC pools estimated by the two classical methods were so different in size (*i.e.* the labile SOC pool estimated as respired-C was about an order of magnitude smaller

than the one estimated as POM-C; Table 1) that it is not surprising that the correlation did not hold specifically when introducing a lot of inter-sites variability. This constitutes another explanation to the lack of correlation between these two indicators of the size of the labile C pool. The two methods appeared to measure different SOC fractions (*i.e.* different sizes) (Table 2 and Fig. 2) that correspond to different SOC lability (*i.e.* mean residence time).

4.2. Relationships between RE6 parameters and POM-C and respired-C

Our RE6 results agreed with previous observations of thermal indicators of SOC lability. For instance, Sebag et al. (2016) reported a trend of decreasing HI and increasing OI_{RE6} with soil depth. Trends of decreasing HI and increasing $T_{50\_CO2\_OX}$ were observed with increasing time since beginning of bare fallow experiments, which corresponded with a progressive decomposition of the labile SOC pool (Barré et al., 2016).

Our correlations between the RE6 parameters and the POM-C fraction were close to those previously reported by Saenger et al. (2015). They indeed obtained a moderate positive correlation ($R^2 = 0.50$) between the labile SOC pool stocks derived from a SOC fractionation scheme isolating POM-C, and the thermally labile SOC pool stocks derived from RE6 indices. We found a similar strong positive correlation between the proportion of labile SOC (1−R-index) and POM-C. The strong relationship between $T_{50\_HC\_PYR}$ and R-index could likely be explained as $T_{50\_HC\_PYR}$ for our samples were very close to the 400 °C threshold used for the calculation of the R-index. As hypothesized we were able to derive a quantitative relationship between some of our RE6 parameters and POM-C (Fig. SI-B1 b–d). The best model was obtained for $T_{50\_HC\_PYR}$ ($R^2 = 0.52$; Fig. 3), while HI, R-index and OI_{RE6} were still moderately good predictors of POM-C ($R^2 = 0.42–0.47$ (Fig. SI-B1 b–d).

Nevertheless no strong relationship between respired-C and the other parameters could be established. Our correlations between the RE6 parameters and respired-C were smaller than

those previously reported by Gregorich et al. (2015). This could be explained by the fact that their study was, by design, very restricted in terms of its soil properties variability and also only considered surface soils (0–10 cm), in which the C/N ratios were around 10.

Previous studies have also demonstrated that RE6 can be used to look at changes in the size of the SOC labile pools with time. For instance, RE6 was able to describe the decrease in the labile SOC pool in long-term bare fallows (Barré et al., 2016). Besides, RE6 captured differences in the size of the labile SOC pools in various land-uses and soil types over a small landscape (Saenger et al., 2015). Our results thus contradict the conclusions from Schiedung et al. (2017) who found no relationship between the thermally labile SOC (200–400 °C) and the C in the POM fractions. The latter (free and occluded POM—obtained by sonication) were indeed more stable at lower oxidation temperatures (300–350 °C) than the mineral-associated fraction. However, their analytical method was different from RE6 protocols: the thermal analysis they used was entirely realized under aerobic conditions (oxidation only), their temperature range was limited (only up to 400 °C) and they used a 50–100 °C temperature step every 15 minutes rather than a constant thermal ramping rate (standard in most thermal studies). For all these reasons, it is likely that their thermal indices differ greatly from our RE6-derived parameters. Moreover their study was based on topsoils (0–10 cm) of only three study sites.

The good approximation of the POM-C fraction by RE6 we reported constitutes a very promising result. POM-C mean residence time (< 20 years in temperate conditions in the absence of an important charcoals contribution; *e.g.*, Trumbore and Zheng, 1996; Balesdent, 1996; Balesdent et al., 1998; Baisden et al., 2002; Schrumpf and Kaiser, 2015) and its size (11 to 23% of total SOC in this study) are much larger than the one of the respired-C fraction, and is thus more meaningful regarding SOC stock evolutions upon changes of land management.

452 This suggests that RE6 could be used to determine the size of the labile SOC pool with a
453 decadal mean residence time.
454
455 4.3. Effects of depth on correlations between the three methods estimating labile SOC
456 Labile SOC content usually decreases with depth (*e.g.*, Lorenz and Lal, 2005; Jenkinson et al.,
457 2008). Such a trend was observed with the three methods used in the present study. Indeed,
458 with depth, we observed a decrease in respired-C (respiration test), POM-C (POM
459 fractionation) and HI alongside with an increase in $T_{50\_HC\_PYR}$ and R-index that all signified
460 the expected decrease in the size the labile SOC pool. Concurrently, OI_{RE6} increased with
461 depth, confirming the increase in SOC oxidative state with increasing decomposition
462 (Hockaday et al., 2009; von Lützow and Kögel-Knabner, 2010; Hockaday et al., 2015).
463 But more importantly, depth affected the correlations between the methods. The lack of
464 correlation between two classical indicators of the labile SOC fraction previously mentioned
465 appeared to originate from opposite trends in the surface and deep layers. In the 0–10 cm
466 layer we observed a surprising negative (but weak) correlation between respired-C and POM-
467 C while the expected positive and moderate correlation between the two indicators was found
468 only in the deep layers. The differences in the sign of the correlations between respired-C and
469 POM-C in the two considered layers (0–10 cm and 40–80 cm) may be related to pedological
470 factors that can limit SOC mineralization in surface horizons. Indeed, the high C/N ratio
471 found in the surface layer (Table SI-A1) is far from the expected C/N of the microorganisms
472 and this lack of N may limit SOC respiration. Similarly, surface layers are on average more
473 acidic (Table SI-A1) than deep layers which can also reduce SOC respiration. We could
474 hypothesize that respired-C and POM-C correlate only when environmental conditions do not
475 limit SOC mineralization explaining the absence of correlation in the acidic N-poor 0–10 cm
476 layer. The significant correlations observed between respired-C and the C/N ratio, pH and the

clay content in the surface layer (Table 2) supports that hypothesis. This opposite behavior in the two layers also affected $T_{50\_HC\_PYR}$, which was not significantly correlated to respired-C in the surface layer while the two parameters were moderately and negatively correlated in the 40–80 cm layer (Table 2). These observations matched those from Peltre et al. (2013) who reported conflicting relationships between the parameter DSC-T50 (temperature at which half of the energy is released in differential scanning calorimetry) and mean soil respiration rates in two sets of high and low SOC content. Their DSC-T50 values were indeed negatively correlated with the respiration values for the low-C soils, whereas there was only a marginal positive correlation between the two parameters for the high-C soils. Their two groups were characterized by soil properties similar to our 0–10 and 40–80 cm layers: their low-C set consisted of samples with a higher pH and lower mean C/N ratio than those of the high-C. Similarly to our 0–10 cm samples, soils in their high-C set had a greater C concentration than those in the low-C set for similar clay contents (Table SI-A1). This would also explain why our results differ from those of Gregorich et al. (2015). In the deep layer, in which the C/N ratios are closer to those reported by Gregorich et al. (2015), we observed the same positive correlation they reported albeit less strong.

Vegetation and soil types did not seem to have affected the correlations between the three methods we tested as much as depth did. However, these environmental factors are likely drivers of the size labile SOC pool as they have been shown to significantly influence RE6 parameters (*e.g.*, Disnar et al., 2003; Sebag et al., 2006).

4.4. Towards high-throughput information on SOC biogeochemical stability using RE6 analysis

Respiration tests and POM fractionation schemes are both time consuming, thus limiting the number of samples and/or replicates that are analyzed. With the RE6 set-up used in this study,

about 20 samples per day can be analyzed, and it requires only limited operator interventions (soil weighing and routine supervision of the RE6 analyzer).

The lack of normalization in many studies using respiration tests and POM fractionation is an important issue and it should be recommended for further studies to include normalized data (% of TOC) when presenting their results. Moreover, despite the fact that POM-C and respired-C are considered as standard estimates of the labile SOC pool, the temperature and/or duration of incubations often varied from one study to the other. Similarly for the POM-C fraction, the density of the solution used for the flotation may drastically differ among studies. This makes data comparison almost impossible. In that regard, while the harmonization of RE6 programs would probably be much easier to implement than respiration tests or POM fractionation protocols as the number of users is still limited, protocol standardization is an important and pressing goal to achieve and this rather quickly as the method starts to gain interest.

RE6 analysis is thus a rapid technique that captures differences in the labile SOC pool as well as other classical techniques. While the understanding of the underlying processes linking SOC thermal stability observed with RE6 and the laboratory or *in-situ* biogeochemical stability of SOC is not fully uncovered and further studies are needed, RE6 analysis appears like a very promising method to provide quick and inexpensive information on the labile SOC pool. Hence, it could constitute a standard method to complement C stock measurements in soil monitoring programs.

Acknowledgments

This work was supported by the Agence de l'environnement et de la maîtrise de l'énergie (ADEME) [APR REACCTIF, piCaSo project] and Campus France [PRESTIGE-2015-3-

0008]. We thank M. Bryant, S. Cecchini, L. Le Vagueresse, J. Mériguet and F. Savignac and for their technical support. The authors acknowledge two anonymous reviewers for their time and valuable comments on the manuscript.

Reference list

Albrecht, R., Sebag, D., Verrecchia, E., 2015. Organic matter decomposition: Bridging the gap between Rock-Eval pyrolysis and chemical characterization (CPMAS ^{13}C NMR). Biogeochemistry 122, 101–111.

Alvarez, R., Alvarez, C.R., 2000. Soil organic matter pools and their associations with carbon mineralization kinetics. Soil Science Society of America Journal 64, 184–189.

Baisden, W.T., Amundson, R., Cook, A.C., Brenner, D.L., 2002. Turnover and storage of C and N in five density fractions from California annual grassland surface soils. Global Biogeochemical Cycles 16, 64-61; 64–16.

Balesdent, J., 1996. The significance of organic separates to carbon dynamics and its modelling in some cultivated soils. European Journal of Soil Science 47, 485–494.

Balesdent, J., Besnard, E., Arrouays, D., Chenu, C., 1998. The dynamics of carbon in particle-size fractions of soil in a forest-cultivation sequence. Plant and Soil 201, 49–57.

Barré, P., Plante, A.F., Cécillon, L., Lutfalla, S., Baudin, F., Christensen, B.T., Eglin, T., Fernandez, J.M., Houot, S., Kätterer, T., Le Guillou, C., Macdonald, A., van Oort, F., Chenu, C., 2016. The energetic and chemical signatures of persistent soil organic matter. Biogeochemistry 130, 1–12.

Behar, F., Beaumont, V., Penteado, D.B., 2001. Rock-Eval 6 technology: Performances and developments. Oil & Gas Science and Technology - Rev.IFP 56, 111–134.

Beleites, C., Sergo, V., 2015. hyperSpec: A Package to Handle Hyperspectral Data Sets in R.

552 Borchers, H.W., 2015. Pracma: Practical numerical math functions.
553 Brêthes, A., Ulrich, E., Lanier, M., 1997. RENECOFOR : Caractéristiques Pédologiques Des
554 102 Peuplements Du Réseau : Observations De 1994/95. Office national des forêts,
555 Département des recherches techniques, Fontainebleau, France, 573 pp.
556 Campbell, C.A., Biederbeck, V.O., Wen, G., Zentner, R.P., Schoenau, J., Hahn, D., 1999a.
557 Seasonal trends in selected soil biochemical attributes: Effects of crop rotation in the
558 semiarid prairie. Canadian Journal of Soil Science 79, 73–84.
559 Campbell, C.A., Lafond, G.P., Biederbeck, V.O., Wen, G., Schoenau, J., Hahn, D., 1999b.
560 Seasonal trends in soil biochemical attributes: Effects of crop management on a black
561 chernozem. Canadian Journal of Soil Science 79, 85–97.
562 Copard, Y., Di-Giovanni, C., Martaud, T., Albéric, P., Olivier, J., 2006. Using Rock-Eval 6
563 pyrolysis for tracking fossil organic carbon in modern environments: Implications for the
564 roles of erosion and weathering. Earth Surface Processes and Landforms 31, 135–153.
565 Crow, S.E., Swanston, C.W., Lajtha, K., Brooks, J.R., Keirstead, H., 2007. Density
566 fractionation of forest soils: Methodological questions and interpretation of incubation
567 results and turnover time in an ecosystem context. Biogeochemistry 85, 69–90.
568 Di-Giovanni, C., Disnar, J.R., Bichet, V., Campy, M., Guillet, B., 1998. Geochemical
569 characterization of soil organic matter and variability of a postglacial detrital organic supply
570 (Chaillexon lake, France). Earth Surface Processes and Landforms 23, 1057–1069.
571 Disnar, J.-R., Guillet, B., Keravis, D., Di-Giovanni, C., Sebag, D., 2003. Soil organic matter
572 (SOM) characterization by Rock-Eval pyrolysis: Scope and limitations. Organic
573 Geochemistry 34, 327–343.
574 Feng, W., Shi, Z., Jiang, J., Xia, J., Liang, J., Zhou, J., Luo, Y., 2016. Methodological
575 uncertainty in estimating carbon turnover times of soil fractions. Soil Biology and
576 Biochemistry 100, 118–124.

577 Gillespie, A.W., Sanei, H., Diochon, A., Ellert, B.H., Regier, T.Z., Chevrier, D., Dynes, J.J.,
578 Tarnocai, C., Gregorich, E.G., 2014. Perennially and annually frozen soil carbon differ in
579 their susceptibility to decomposition: Analysis of subarctic earth hummocks by bioassay,
580 XANES and pyrolysis. Soil Biology and Biochemistry 68, 106–116.
581 Golchin, A., Oades, J.M., Skjemstad, J.O., Clarke, P., 1994. Study of free and occluded
582 particulate organic matter in soils by solid state ^{13}C CP/MAS NMR spectroscopy and
583 scanning electron microscopy. Australian Journal of Soil Research 32, 285–309.
584 Gregorich, E.G., Gillespie, A.W., Beare, M.H., Curtin, D., Sanei, H., Yanni, S.F., 2015.
585 Evaluating biodegradability of soil organic matter by its thermal stability and chemical
586 composition. Soil Biology and Biochemistry 91, 182–191.
587 Harrell, F.E.J., Dupont, C., and others, 2016. Hmisc: Harrell miscellaneous.
588 Harris, D., Horwáth, W.R., van Kessel, C., 2001. Acid fumigation of soils to remove
589 carbonates prior to total organic carbon or CARBON-13 isotopic analysis. Soil Science
590 Society of America Journal 65, 1853–1856.
591 Hassan, W., Bashir, S., Ahmed, N., Tanveer, M., Shah, A.N., Bano, R., David, J., 2016.
592 Labile organic carbon fractions, regulator of CO_2 emission: Effect of plant residues and
593 water regimes. CLEAN - Soil, Air, Water 44, 1358–1367.
594 Hassink, J., 1995. Density fractions of soil macroorganic matter and microbial biomass as
595 predictors of C and N mineralization. Soil Biology and Biochemistry 27, 1099–1108.
596 Haynes, R.J., 1986. Chapter 2 - the Decomposition Process: Mineralization, Immobilization,
597 Humus Formation, and Degradation. In: Haynes, R.J. (Ed.), Mineral Nitrogen in the Plant–
598 Soil System. Academic Press, pp. 52–126.
599 Haynes, R.J., 2005. Labile organic matter fractions as central components of the quality of
600 agricultural soils: An overview. Advances in Agronomy 85, 221–268.

601 Hetényi, M., Nyilas, T., Sajgó, C., Brukner-Wein, A., 2006. Heterogeneous organic matter
602 from the surface horizon of a temperate zone marsh. Organic Geochemistry 37, 1931–1942.
603 Hetényi, M., Nyilas, T., Tóth, T.M., 2005. Stepwise Rock-Eval pyrolysis as a tool for typing
604 heterogeneous organic matter in soils. Journal of Analytical and Applied Pyrolysis 74, 45–
605 54.
606 Hockaday, W.C., Gallagher, M.E., Masiello, C.A., Baldock, J.A., Iversen, C.M., Norby, R.J.,
607 2015. Forest soil carbon oxidation state and oxidative ratio responses to elevated CO_2.
608 Journal of Geophysical Research: Biogeosciences 120, 1797–1811.
609 Hockaday, W.C., Masiello, C.A., Randerson, J.T., Smernik, R.J., Baldock, J.A., Chadwick,
610 O.A., Harden, J.W., 2009. Measurement of soil carbon oxidation state and oxidative ratio by
611 ^{13}C nuclear magnetic resonance. Journal of Geophysical Research 114.
612 IUSS Working Group, 2015. World reference base for soil resources 2014 (update 2015),
613 international soil classification system for naming soils and creating legends for soil maps.
614 World Soil Resources Reports No. 106. FAO, Rome.
615 Janzen, H.H., Campbell, C.A., Brandt, S.A., Lafond, G.P., Townley-Smith, L., 1992. Light-
616 fraction organic matter in soils from long-term crop rotations. Soil Science Society of
617 America Journal 56, 1799–1806.
618 Jenkinson, D.S., Poulton, P.R., Bryant, C., 2008. The turnover of organic carbon in subsoils.
619 Part 1. Natural and bomb radiocarbon in soil profiles from the Rothamsted long-term field
620 experiments. European Journal of Soil Science 59, 391–399.
621 Jonard, M., Nicolas, M., Coomes, D.A., Caignet, I., Saenger, A., Ponette, Q., 2017. Forest
622 soils in France are sequestering substantial amounts of carbon. Science of The Total
623 Environment 574, 616–628.
624 Kassambara, A., Mundt, F., 2016. Factoextra: Extract and visualize the results of multivariate
625 data analyses.

626 Lafargue, E., Marquis, F., Pillot, D., 1998. Rock-Eval 6 applications in hydrocarbon
627 exploration, production, and soil contamination studies. Oil & Gas Science and Technology
628 - Revue IFP 53, 421–437.
629 Li, X.J., Li, X.R., Wang, X.P., Yang, H.T., 2016. Changes in soil organic carbon fractions
630 after afforestation with xerophytic shrubs in the tengger desert, northern china. European
631 Journal of Soil Science 67, 184–195.
632 Liang, B.C., McConkey, B.G., Schoenau, J., Curtin, D., Campbell, C.A., Moulin, A.P.,
633 Lafond, G.P., Brandt, S.A., Wang, H., 2003. Effect of tillage and crop rotations on the light
634 fraction organic carbon and carbon mineralization in chernozemic soils of Saskatchewan.
635 Canadian Journal of Soil Science 83, 65–72.
636 Lorenz, K., Lal, R., 2005. The depth distribution of soil organic carbon in relation to land use
637 and management and the potential of carbon sequestration in subsoil horizons. Advances in
638 Agronomy 88, 35–66.
639 Luo, Y., Ahlström, A., Allison, S.D., Batjes, N.H., Brovkin, V., Carvalhais, N., Chappell, A.,
640 Ciais, P., Davidson, E.A., Finzi, A., Georgiou, K., Guenet, B., Hararuk, O., Harden, J.W.,
641 He, Y., Hopkins, F., Jiang, L., Koven, C., Jackson, R.B., Jones, C.D., Lara, M.J., Liang, J.,
642 McGuire, A.D., Parton, W., Peng, C., Randerson, J.T., Salazar, A., Sierra, C.A., Smith, M.J.,
643 Tian, H., Todd-Brown, K.E.O., Torn, M., van Groenigen, K.J., Wang, Y.P., West, T.O.,
644 Wei, Y., Wieder, W.R., Xia, J., Xu, X., Xu, X., Zhou, T., 2016. Toward more realistic
645 projections of soil carbon dynamics by earth system models. Global Biogeochemical Cycles
646 30, 40–56.
647 Peltre, C., Fernández, J.M., Craine, J.M., Plante, A.F., 2013. Relationships between biological
648 and thermal indices of soil organic matter stability differ with soil organic carbon level.
649 SSSAJ 77, 2020–2028.

650 Ponette, Q., Ulrich, E., Brêthes, A., Bonneau, M., Lanier, M., 1997. RENECOFOR - Chimie
651 Des Sols Dans Les 102 Peuplements Du Réseau : Campagne De Mesures 1993-95. ONF,
652 Département des recherches techniques, Fontainebleau, France, 427 pp.
653 R Core Team, 2016. R: A language and environment for statistical computing.
654 Saenger, A., Cécillon, L., Poulenard, J., Bureau, F., De Daniéli, S., Gonzalez, J., Brun, J.,
655 2015. Surveying the carbon pools of mountain soils: A comparison of physical fractionation
656 and Rock-Eval pyrolysis. Geoderma 241–242, 279–288.
657 Schiedung, M., Don, A., Wordell-Dietrich, P., Alcántara, V., Kuner, P., Guggenberger, G.,
658 2017. Thermal oxidation does not fractionate soil organic carbon with differing biological
659 stabilities. Journal of Plant Nutrition and Soil Science 180, 18–26.
660 Schrumpf, M., Kaiser, K., 2015. Large differences in estimates of soil organic carbon
661 turnover in density fractions by using single and repeated radiocarbon inventories.
662 Geoderma 239–240, 168–178.
663 Sebag, D., Disnar, J.R., Guillet, B., Di Giovanni, C., Verrecchia, E.P., Durand, A., 2006.
664 Monitoring organic matter dynamics in soil profiles by 'Rock-Eval pyrolysis': Bulk
665 characterization and quantification of degradation. European Journal of Soil Science 57,
666 344–355.
667 Sebag, D., Verrecchia, E.P., Cécillon, L., Adatte, T., Albrecht, R., Aubert, M., Bureau, F.,
668 Cailleau, G., Copard, Y., Decaens, T., Disnar, J.-R., Hetényi, M., Nyilas, T., Trombino, L.,
669 2016. Dynamics of soil organic matter based on new Rock-Eval indices. Geoderma 284,
670 185–203.
671 Six, J., Elliott, E.T., Paustian, K., Doran, J.W., 1998. Aggregation and soil organic matter
672 accumulation in cultivated and native grassland soils. Soil Science Society of America
673 Journal 62, 1367–1377.

674 Trumbore, S.E., Zheng, S., 1996. Comparison of fractionation methods for soil organic matter
675 ^{14}C analysis. Radiocarbon 38, 219–229.
676 Trumbore, S.E., Chadwick, O.A., Amundson, R., 1996. Rapid exchange between soil carbon
677 and atmospheric carbon dioxide driven by temperature change. Science 272, 393–396.
678 Ulrich, E., 1995. Le réseau RENECOFOR : Objectifs et réalisation. Revue forestière française
679 47, 107–124.
680 von Lützow, M., Kögel-Knabner, I., 2010. Response to the concept paper: 'What is
681 recalcitrant soil organic matter?' by Markus Kleber. Environmental Chemistry 7, 333–335.
682 von Lützow, M., Kögel-Knabner, I., Ekschmitt, K., Flessa, H., Guggenberger, G., Matzner,
683 E., Marschner, B., 2007. SOM fractionation methods: Relevance to functional pools and to
684 stabilization mechanisms. Soil Biology and Biochemistry 39, 2183–2207.
685 Wander, M.M., Bidart, M.G., 2000. Tillage practice influences on the physical protection,
686 bioavailability and composition of particulate organic matter. Biology and Fertility of Soils
687 32, 360–367.
688 Wander, M., 2004. Soil Organic Matter Fractions and their Relevance to Soil Function. In:
689 Magdoff, F., Weil, R.R. (Eds.), Soil Organic Matter in Sustainable Agriculture. CRC Press,
690 pp. 67–102.
691

Figure captions

Fig. 1. (a) Location of the 53 study sites front the French national network for the long term monitoring of forest ecosystems (RENECOFOR); (b) Number of samples by depths and analyses realized. Plot locations are also available via the Interactive Map Viewer.

Fig. 2. Biplot of a principal components analysis (PCA) showing the loadings of the 6 parameters estimating the labile SOC (red arrows) and the 99 soil samples for the two layers (0–10 cm, n = 53; 40–80 cm, n = 46) along the first two principal component axes (PC1 and PC2). The 95% ellipses for both soil layers were added for information; the circle in the center corresponds to the circle of correlations.

Fig. 3. The proportion of OC in the POM fraction (POM-C) as a function of $T_{50\_HC\_PYR}$ (the temperature at which 50% of the HC pyrolysis effluents have evolved) for all samples (n = 99; surface = 0–10 cm and deep = 40–80 cm).

Figure captions

Fig. 1. (a) Location of the 53 study sites front the French national network for the long term monitoring of forest ecosystems (RENECOFOR); (b) Number of samples by depths and analyses realized. Plot locations are also available via the Interactive Map Viewer.

Fig. 2. Biplot of a principal components analysis (PCA) showing the loadings of the 6 parameters estimating the labile SOC (red arrows) and the 99 soil samples for the two layers (0–10 cm, n = 53; 40–80 cm, n = 46) along the first two principal component axes (PC1 and PC2). The 95% ellipses for both soil layers were added for information; the circle in the center corresponds to the circle of correlations.

Fig. 3. The proportion of OC in the POM fraction (POM-C) as a function of $T_{50\_HC\_PYR}$ (the temperature at which 50% of the HC pyrolysis effluents have evolved) for all samples (n = 99; surface = 0–10 cm and deep = 40–80 cm).

Table 1

Table 1. Mean (and minimum; maximum; standard deviation) of the RE6 (HI, OI_{RE6}, $T_{50\_HC\_PYR}$, $T_{50\_CO2\_OX}$, R-index, I-index), respiration test (10-week mineralizable C, respired-C) and POM fractionation (POM-C) parameters, as well as the bulk SOC content for each soil layer (0–10 and 40–80 cm) of the 53 RENECOFOR plots.

	n	HI (mg HC / g TOC)	OI_{RE6} (mg O_2 / g TOC)	$T_{50\_HC\_PYR}$ (°C)	$T_{50\_CO2\_OX}$ (°C)	R-index (% SOC)	I-index	Respired-C (mg CO_2-C / g SOC)	POM-C (% SOC)	SOC (%) (bulk soil)
0–10 cm	53	276 (161; 443; 77)	225 (161; 288; 37)	421 (400; 439; 9)	399 (382; 422; 9)	59 (50; 68; 4)	0.17 (0.00; 0.32; 0.07)	17.0 (4.4; 33.7; 7.2)	22.6 (12.1; 43.0; 7.3)	5.1 (1.2; 15.1; 2.7)
40–80 cm	46	133 (75; 202; 34)	439 (236; 875; 138)	448 (421; 480; 10)	431 (390; 470; 18)	69 (59; 79; 5)	0.11 (−0.18; 0.39; 0.14)	13.4 (3.6; 32.2; 6.9)	11.0 (2.5; 33.6; 6.1)	0.9 (0.2; 3.9; 0.8)

Table 2

Table 2. Spearman correlation coefficients between 10-week mineralizable SOC (respired-C), the proportion of OC in the POM fraction (POM-C), the RE6 parameters and the C/N ratio, pH and clay content of the bulk soil, for both the 0–10 cm (n = 53) and 40–80 cm (n = 46) layers and each layer individually. Significance is indicated as follows: ***: $p < 0.001$; **: $p < 0.01$; *: $p < 0.05$. The very high correlations are marked in bold.

All (n = 99)	respired-C	POM-C	$T_{50\_HC\_PYR}$	$T_{50\_CO2\_OX}$	HI	OI_{RE6}	I-index	R-index	C/N	pH
POM-C	0.20									
$T_{50\_HC\_PYR}$	−0.26**	−0.73***								
$T_{50\_CO2\_OX}$	−0.16	−0.56***	0.76***							
HI	0.06	0.67***	−0.78***	−0.66***						
OI_{RE6}	−0.02	−0.76***	0.78***	0.63***	**−0.92*****					
I-index	0.32**	0.35***	−0.48***	−0.17	0.10	0.06				
R-index	−0.31**	−0.69***	**0.93*****	0.64***	−0.64***	0.67***	−0.74***			
C/N	−0.13	0.63***	−0.55***	−0.52***	0.67***	−0.78***	0.16	−0.50***		
pH	0.23*	−0.55***	0.49***	0.44***	−0.57***	0.66***	−0.27**	0.49***	−0.64***	
clay content	0.20	−0.19	0.04	−0.06	−0.17	0.31**	−0.22**	0.13	−0.49***	0.43***
0–10 cm	respired-C	POM-C	$T_{50\_HC\_PYR}$	$T_{50\_CO2\_OX}$	HI	OI_{RE6}	I-index	R-index	C/N	pH
POM-C	−0.29*									
$T_{50\_HC\_PYR}$	0.12	−0.44***								
$T_{50\_CO2\_OX}$	0.13	−0.19	0.45***							
HI	−0.43**	0.32*	−0.30*	0.07						
OI_{RE6}	0.52***	−0.41**	0.40**	−0.06	−0.91***					
I-index	0.11	0.37**	−0.87***	−0.43**	0.04	−0.17				
R-index	0.07	−0.44**	**0.99*****	0.44***	−0.24	−0.35*	**−0.92*****			
C/N	−0.51***	0.56***	−0.55***	−0.19	0.67***	−0.80***	0.37**	−0.52***		
pH	0.62***	−0.35**	0.46***	0.36**	−0.61***	0.70***	−0.25	0.42**	−0.70***	
clay content	0.43**	−0.29*	0.44**	−0.03	−0.71***	0.75***	−0.31*	0.43**	−0.70***	0.60***

40–80 cm	respired−C	POM−C	$T_{50\_HC\_PYR}$	$T_{50\_CO2\_OX}$	HI	OI_{RE6}	I−index	R-index	C/N	pH
POM−C	0.47***									
$T_{50\_HC\_PYR}$	−0.41**	−0.35*								
$T_{50\_CO2\_OX}$	−0.01	−0.01	0.26							
HI	−0.03	0.06	−0.24	−0.24						
OI_{RE6}	0.13	−0.42**	0.10	0.22	−0.47***					
I−index	0.41**	0.13	−0.19	0.43**	−0.49***	0.40**				
R-index	−0.52***	−0.28	0.64***	−0.19	0.20	−0.20	−0.85***			
C/N	−0.17	0.30*	0.10	−0.18	0.25	−0.65***	0.30*	0.23		
pH	0.03	−0.34*	−0.03	−0.18	0.11	0.25	−0.07	0.06	−0.27	
clay content	−0.08	−0.42**	−0.01	0.11	−0.07	0.62***	−0.15	0.17	−0.59***	0.35*

Figure 1

Click here to download high resolution image

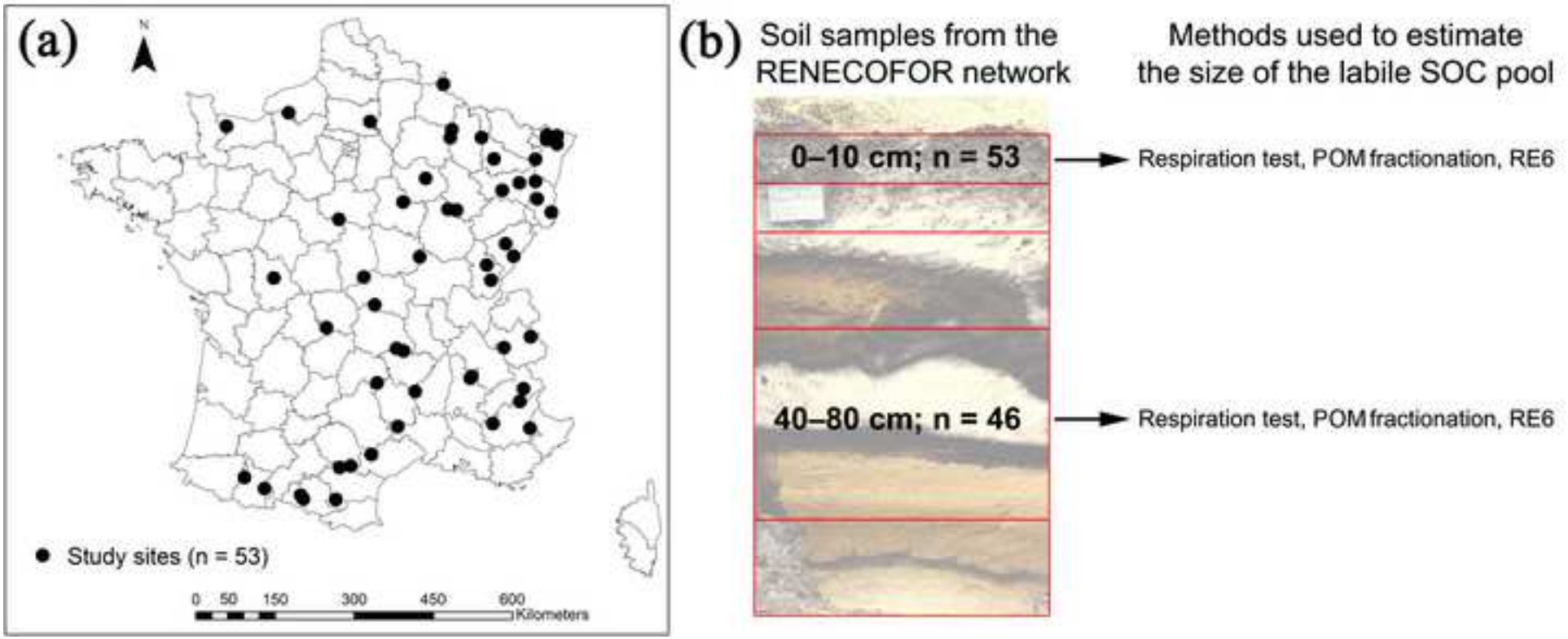

Figure 2

Click here to download high resolution image

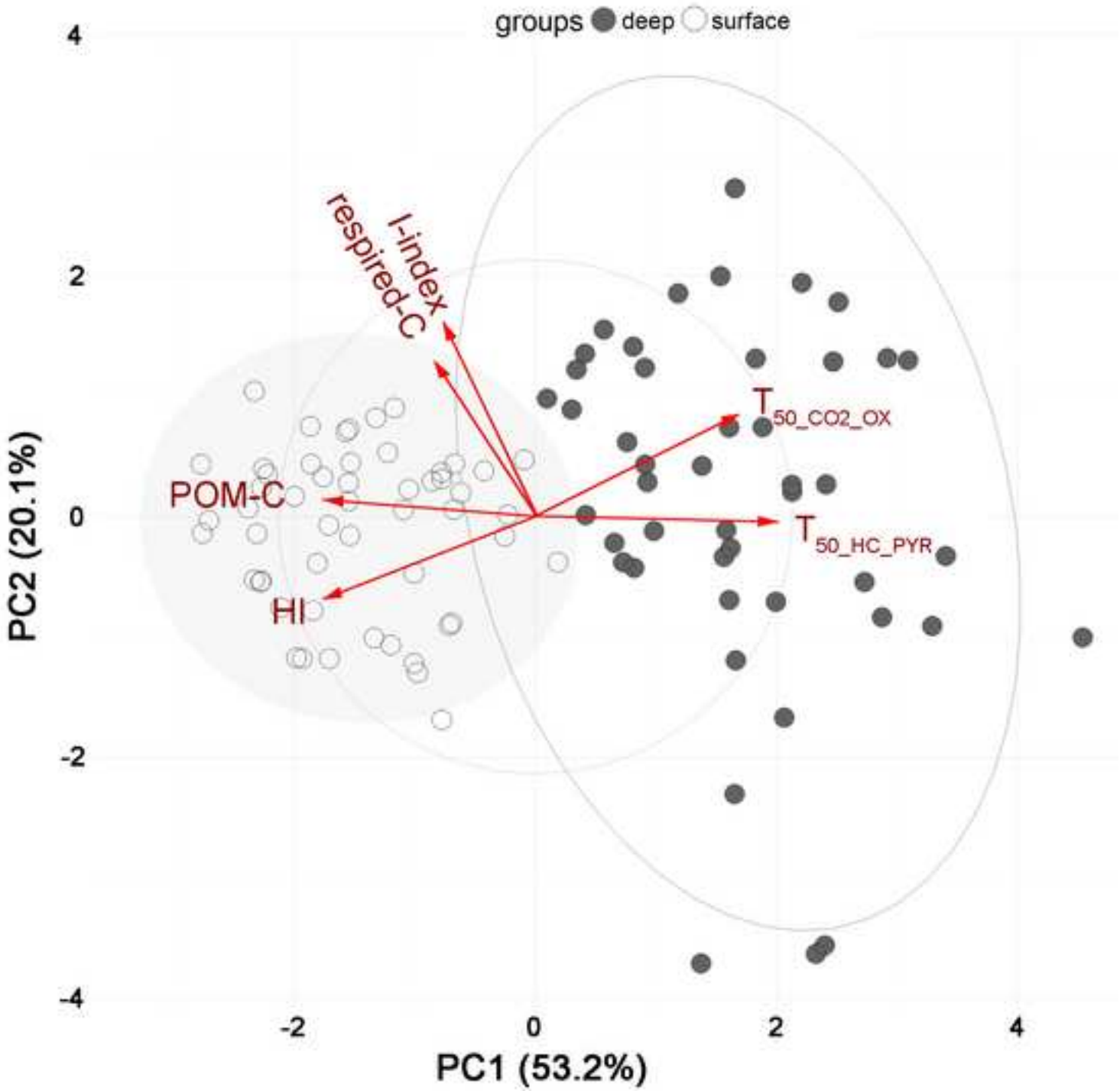

Figure 3

Click here to download high resolution image

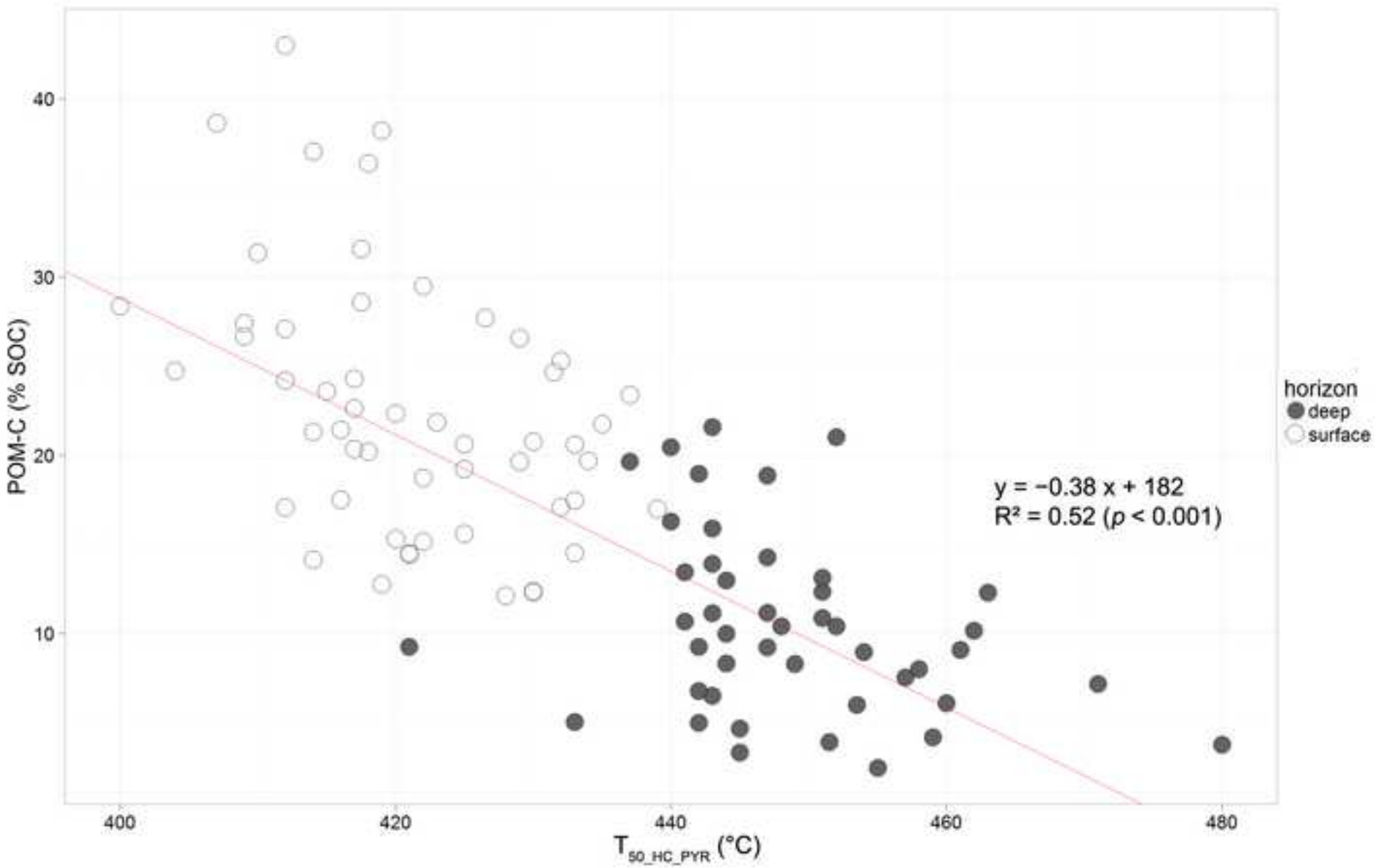

Is Rock-Eval 6 thermal analysis a good indicator of soil organic carbon lability? – A method-comparison study in forest soils

Laure Soucémarianadin[1,*], Lauric Cécillon[2], Claire Chenu[3], François Baudin[4], Manuel Nicolas[5], Cyril Girardin[3] and Pierre Barré[1]

Supporting Information

Table SI-A.1. Mean (+ standard deviation) particle-size distribution, pH and C/N ratio of the studied samples.

Table SI-B1. Percentage of variance explained and loadings of the first three principal components (PC) after Box-Cox transformation to correct for skewness for the PCA of all (0–10 cm and 40–80 cm) samples (n = 99). Values in bold indicate the variables with loading greater than the mean of the absolute loading in each PC.

Table SI-C1. Spearman correlation coefficients between 10-week mineralizable SOC (respired-C), the proportion of OC in the POM fraction (POM-C), the RE6 parameters and the C/N ratio of the bulk soil, for the three soil types and the two vegetation types. Significance is indicated as follows: ***: $p < 0.001$; **: $p < 0.01$; *: $p < 0.05$. The very high (> 0.9) correlations are marked in bold.

Fig. SI-A1. Description of the Rock-Eval 6 thermal analysis (adapted from Saenger et al., 2013) and calculation of four RE6-derived parameters (Hydrogen index; Oxygen index; $T_{50\_HC\_PYR}$, the temperature at which 50% of the HC resulting from the SOM pyrolysis had

evolved; $T_{50\_CO2\_OX}$, the temperature at which 50% of the residual SOM was oxidized to CO_2 during the oxidation phase).

Fig. SI-B1. The proportion of OC in the POM fraction (POM-C) as a function of (a) respired-C (the proportion of total SOC mineralizable during a 10-week laboratory incubation); (b) OI_{RE6} (the oxygen index); (c) HI (the hydrogen index); (d) R-index (the proportion of thermally stable SOC pool) for all samples (n = 99; surface = 0–10 cm and deep = 40–80 cm).

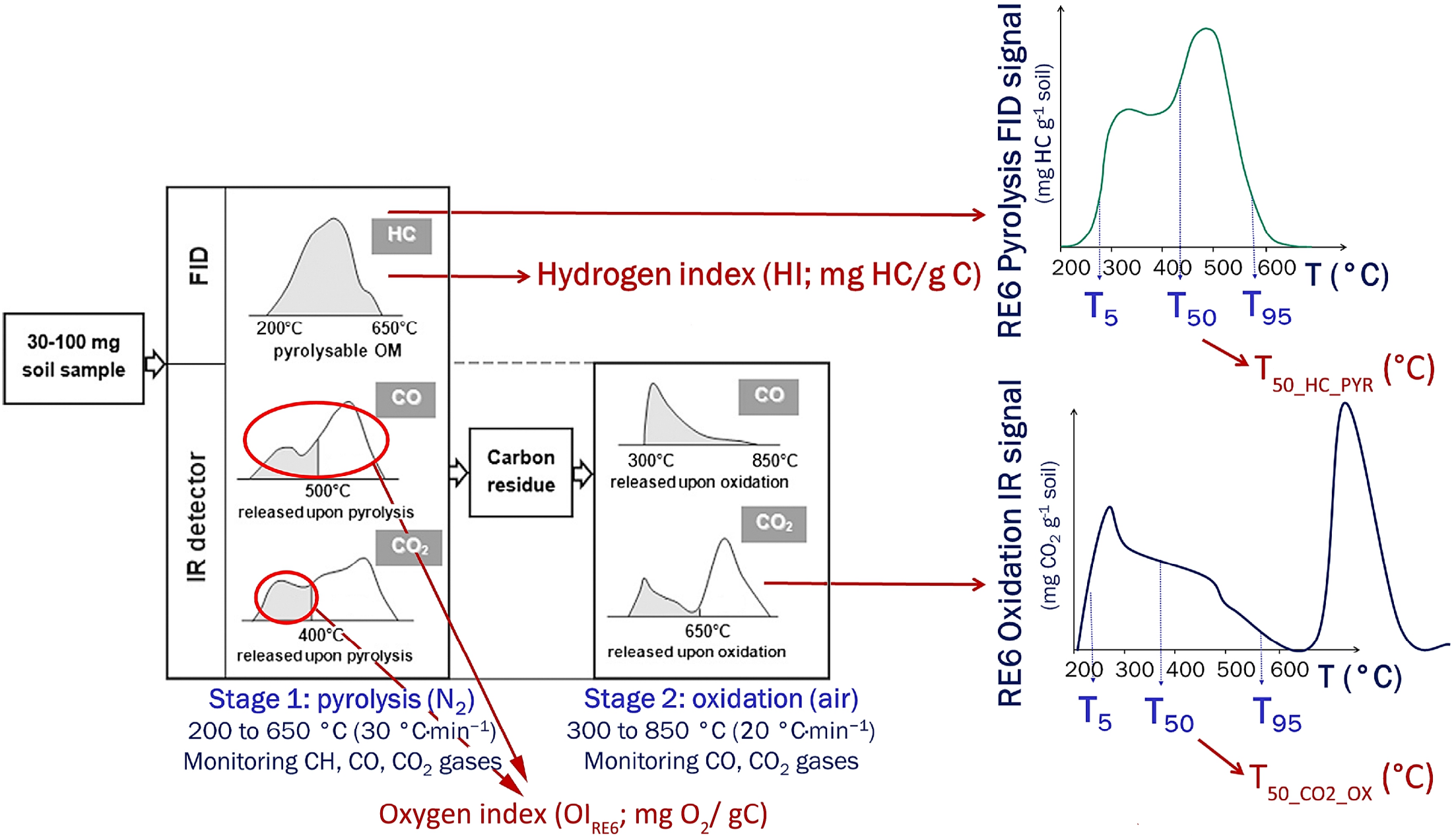
30-100 mg soil sample
FID
IR detector
HC
200°C
650°C
pyrolysable OM
CO
500°C
released upon pyrolysis
CO2
400°C
released upon pyrolysis
Carbon residue
CO
300°C
850°C
released upon oxidation
CO2
650°C
released upon oxidation
Hydrogen index (HI; mg HC/g C)
Oxygen index (OIRE6; mg O2/ gC)
Stage 1: pyrolysis (N2)
200 to 650 °C (30 °C·min-1)
Monitoring CH, CO, CO2 gases
Stage 2: oxidation (air)
300 to 850 °C (20 °C·min-1)
Monitoring CO, CO2 gases
RE6 Pyrolysis FID signal
(mg HC g-1 soil)
200 300 400 500 600 T (°C)
T5 T50 T95
T50_HC_PYR (°C)
RE6 Oxidation IR signal
(mg CO2 g-1 soil)
200 300 400 500 600 T (°C)
T5 T50 T95
T50_CO2_OX (°C)

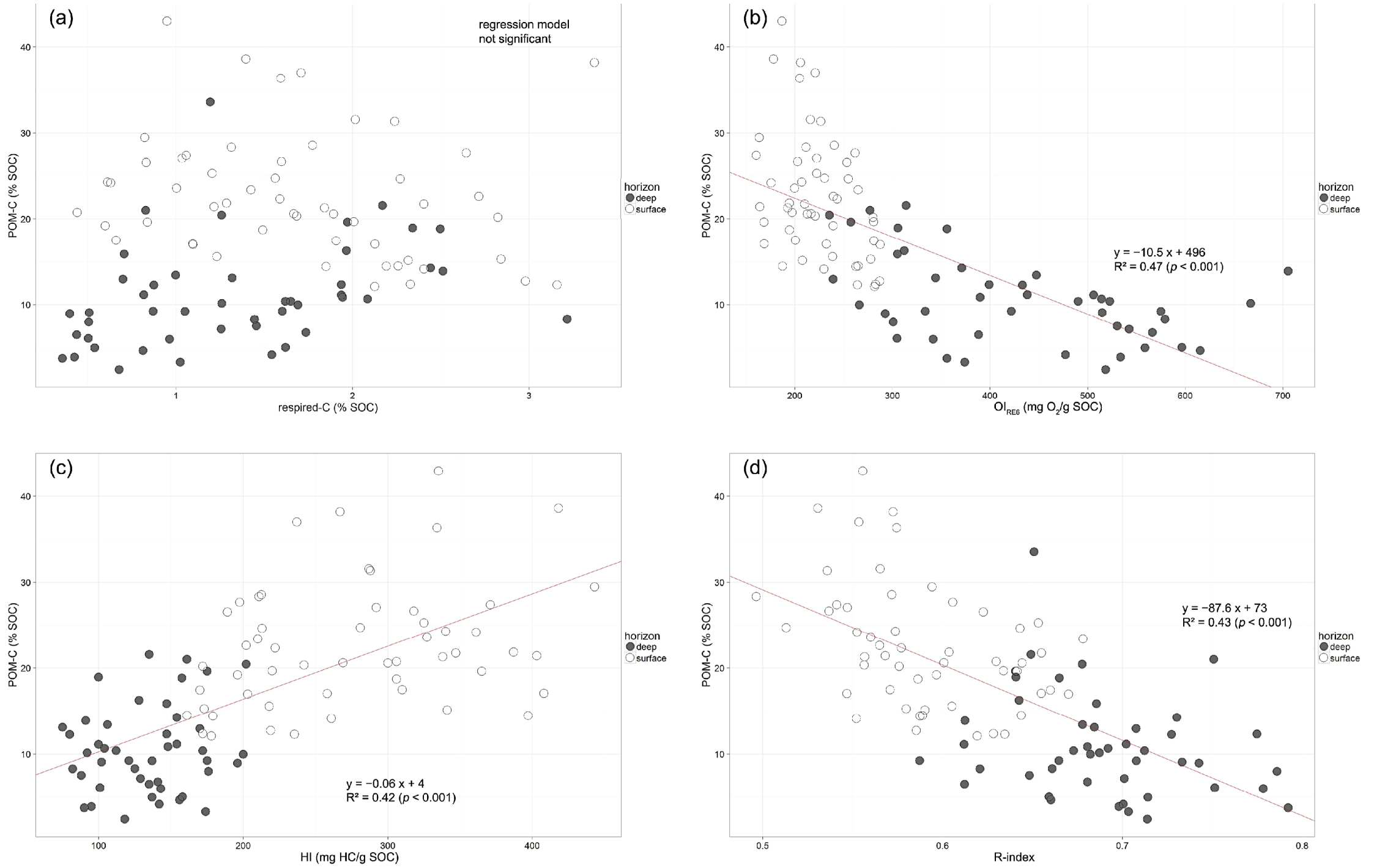
(a)
regression model
not significant
POM-C (% SOC)
respired-C (% SOC)
horizon
deep
surface
(b)
y = −10.5 x + 496
R² = 0.47 (p < 0.001)
OI_RE6 (mg O2/g SOC)
(c)
y = −0.06 x + 4
R² = 0.42 (p < 0.001)
HI (mg HC/g SOC)
(d)
y = −87.6 x + 73
R² = 0.43 (p < 0.001)
R-index

Table SI-A.1. Mean (+ standard deviation) particle-size distribution, pH and C/N ratio of the studied samples in each layer of the 53 plots.

depth (cm)	n	clay (%)		silt (%)		sand (%)		pH_{water}		C/N bulk soil	
0–10	53	22.5	(13.6)	35.5	(18.0)	42.0	(28.8)	4.9	(1.0)	16.9	(4.5)
40–80	46	21.0	(15.4)	32.8	(16.2)	46.2	(26.7)	5.9	(1.5)	11.8	(3.8)

Table SI-B1. Percentage of variance explained and loadings of the first three principal components (PC) after Box-Cox transformation to correct for skewness for the PCA of all samples (n = 99). Values in bold indicate the variables with loading greater than the mean of the absolute loading in each PC.

PC	PC1	PC2	PC3
% variance explained	53.2	20.1	13.1
respired-C	−0.22	**0.55**	**0.77**
POM-C	**−0.47**	0.06	0.00
$T_{50\_HC\_PYR}$	**0.53**	−0.02	0.11
$T_{50\_CO2\_OX}$	**0.45**	**0.36**	−0.18
HI	**−0.46**	−0.29	−0.15
I-index	−0.20	**0.69**	**−0.58**

Table SI-C1. Spearman correlation coefficients between 10-week mineralizable SOC (respired-C), the proportion of OC in the POM fraction (POM-C), the RE6 parameters and the C/N ratio of the bulk soil, for the three soil types and the two vegetation types. Significance is indicated as follows: ***: $p < 0.001$; **: $p < 0.01$; *: $p < 0.05$. The very high (> 0.9) correlations are marked in bold.

		SOIL TYPE									
		respired-C	POM-C	$T_{50\_HC\_PYR}$	$T_{50\_CO2\_OX}$	HI	I-index	OI_{RE6}	R-index	C/N	pH
dystric Cambisol	POM-C	0.15									
	$T_{50\_HC\_PYR}$	−0.36*	−0.68***								
	$T_{50\_CO2\_OX}$	−0.18	−0.67***	0.77***							
	HI	0.17	0.62***	−0.81***	−0.65***						
	I-index	0.47**	−0.01	−0.20	0.05	−0.17					
	OI_{RE6}	−0.15	−0.73***	0.82***	0.73***	−0.89***	0.15				
	R-index	−0.50**	−0.52**	**0.90****	0.61***	−0.62***	−0.58***	0.63***			
	C/N	0.11	0.68***	−0.67***	−0.66***	0.58***	0.14	−0.75***	−0.64***		
	pH	0.14	−0.60***	0.58***	0.51**	−0.61***	0.08	0.60***	0.42*	−0.38*	
	clay content	−0.30	−0.16	0.15	−0.02	−0.03	−0.45**	0.23	0.32	−0.27	−0.02
eutric Cambisol	POM-C	0.46*									
	$T_{50\_HC\_PYR}$	−0.45*	−0.68***								
	$T_{50\_CO2\_OX}$	−0.54**	−0.53**	0.77***							
	HI	0.31	0.72***	−0.52**	−0.48**						
	I-index	0.39*	0.37*	−0.58***	−0.36	0.21					
	OI_{RE6}	−0.42*	−0.88***	0.68***	0.55**	−0.83***	−0.39*				
	R-index	−0.50**	−0.68***	**0.94****	0.72***	−0.55**	−0.78***	0.70***			
	C/N	0.41*	0.84***	−0.60***	−0.49**	0.71***	0.17	−0.82***	−0.54**		
	pH	−0.57***	−0.56**	0.69***	0.71***	−0.54**	−0.20	0.62***	0.62***	−0.56**	
	clay content	−0.03	−0.13	−0.08	−0.08	−0.03	−0.14	−0.05	0.01	0.01	−0.25
entic Podzol	POM-C	0.42*									
	$T_{50\_HC\_PYR}$	−0.35*	−0.86***								
	$T_{50\_CO2\_OX}$	−0.24	−0.52**	0.69***							
	HI	0.18	0.71***	−0.75***	−0.57***						
	I-index	0.31	0.55***	−0.69***	−0.30	0.27					
	OI_{RE6}	−0.15	−0.71***	0.75***	0.48**	**−0.96****	−0.26				
	R-index	−0.32	−0.83***	**0.97****	0.62***	−0.68***	−0.81***	0.68***			
	C/N	0.08	0.54**	−0.55***	−0.44*	0.74***	0.13	−0.70***	−0.46**		
	pH	−0.29	−0.69***	0.83***	0.72***	−0.71***	−0.48**	0.72***	0.79***	−0.55***	
	clay content	−0.01	−0.10	−0.06	−0.29	−0.15	0.05	0.23	−0.06	−0.39*	0.02

VEGETATION TYPE

		respired-C	POM-C	$T_{50\_HC\_PYR}$	$T_{50\_CO2\_OX}$	HI	I-index	OI_{RE6}	R-index	C/N	pH
coniferous	POM-C	0.20									
	$T_{50\_HC\_PYR}$	−0.25	−0.67***								
	$T_{50\_CO2\_OX}$	−0.24	−0.52***	0.72***							
	HI	0.05	0.70***	−0.82***	−0.67***						
	I-index	0.29*	0.38**	−0.52***	−0.16	0.21					
	OI_{RE6}	0.00	−0.75***	0.76***	0.58***	**−0.92****	−0.27				
	R-index	−0.25	−0.68***	**0.95****	0.63***	−0.75***	−0.74***	0.74***			
	C/N	−0.13	0.60***	−0.46***	−0.33*	0.73***	0.19	−0.80***	−0.47***		
	pH	0.37**	−0.54***	0.42**	0.37**	−0.64***	−0.18	0.70***	0.45***	−0.66***	
	clay content	0.27*	−0.20	−0.11	−0.32*	−0.15	−0.09	0.33*	−0.01	−0.51***	0.50***
deciduous	POM-C	0.21									
	$T_{50\_HC\_PYR}$	−0.29	−0.80***								
	$T_{50\_CO2\_OX}$	−0.07	−0.56***	0.70***							
	HI	0.10	0.69***	−0.83***	−0.73***						
	I-index	0.40**	0.17	−0.24	0.15	−0.04					
	OI_{RE6}	−0.05	−0.77***	0.84***	0.69***	**−0.92****	0.03				
	R-index	−0.44**	−0.73***	**0.92****	0.52***	−0.66***	−0.57***	0.67***			
	C/N	−0.16	0.67***	−0.66***	−0.66***	0.81***	−0.20	−0.86***	−0.46**		
	pH	0.07	−0.55***	0.52***	0.42**	−0.53***	−0.19	0.60***	0.52***	−0.61***	
	clay content	0.09	−0.12	0.16	0.15	−0.26	−0.25	0.27	0.24	−0.34*	0.35*